

KMS Technologies – KJT Enterprises Inc.

**Chapter 7
General Case Histories**

extract from

Strack, K.-M., 1992, reprinted 1999
***Exploration with deep transient
electromagnetic:*** Elsevier, 373 pp.

This material is not longer cover by copyright. The copyright was released by Elsevier to Dr. Strack on November 5th, 2007.

The author explicit authorizes unrestricted use of this material as long as proper reference is given.

Chapter 7

General Case Histories

In the following chapters several case histories are presented, where LOTEM measurements have been carried out in conjunction with other geophysical techniques available well log information. In this chapter, the case histories not falling under a specific category are listed. These surveys were mostly carried out for test and calibration purposes. The first case history is from the University of Cologne test site north of the Ruhr area in Germany (Stephan, 1989). The survey area is a part of the "Rheinische Schiefergebirge", North-West Germany. The sediments are of upper Carboniferous and more than 5000 m thick. Two historic case studies follow: the geologic calibration of the method with the Group Seven Inc. system near the Colorado School of Mines test area and the first field tests of the method in Australia. The last case history in this chapter describes the first quantitative 3-D interpretation of LOTEM field measurements in the Münsterland Basin, FRG.

FIELD SURVEY NORTH OF THE RUHR DISTRICT, FRG

The test area is located approximately 100 km north of Cologne and about 10 km north of the Ruhr District, one of the most densely populated and industrialized districts in Germany. The area was selected for its closeness to Cologne with the following objectives in mind:

- Due to its closeness to the Ruhr district, the test area shows very strong cultural noise. It is an ideal site to test the noise compensation and data processing techniques developed for the LOTEM system.
- Because of the coal mining activities, the geology of the area is extremely well known. Several logged wells allow the comparison of the method with known geology to overcome these problems.
- In parts of the survey area, reflection seismic measurements have problems due to a thin water bearing layer. Thus a field survey in the area would be a good demonstration of the capability of the LOTEM method.

Figure 7.1 shows the base maps for two surveys carried out during 1987 and 1988. During the 1987 survey, only one transmitter was used in order to reach the above objectives. A total of 145 individual soundings at 100 different receiver locations were recorded. Because no significant resistive layer was expected in the survey area, observations of the time derivative of the magnetic field were sufficient to resolve the resistivity structure (Strack et al, 1989b). During the 1988 survey two different transmitters

were used in order to verify the results from the 1987 survey, and to address the question of repeatability of the field measurements using different systems and different field crews.

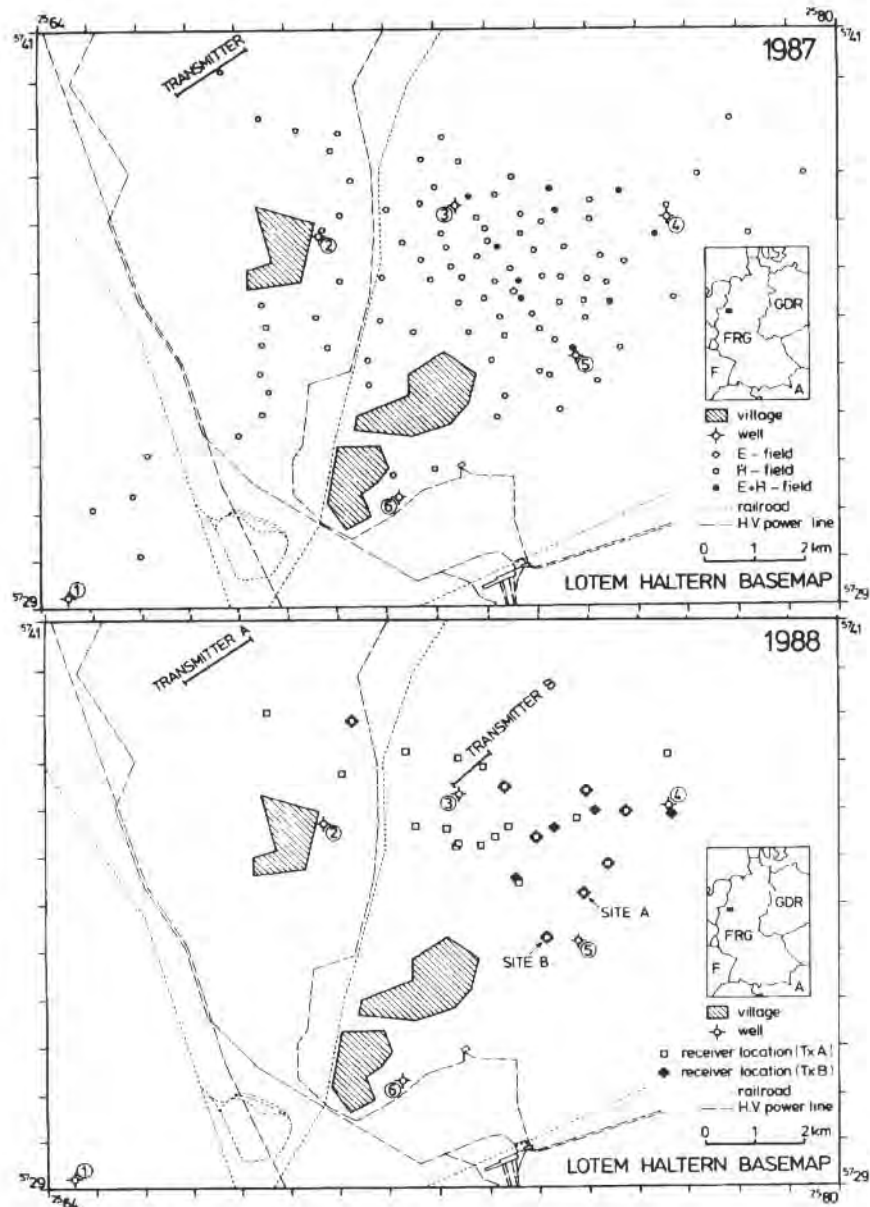


Fig. 7.1: Survey layout of the 1987 (top) and the 1988 (bottom) LOTEM survey.

Additional information from six boreholes was available; their respective locations are shown in figures 7.1. Figure 7.2 shows a representative well log for the area with a conductor sandwiched between two resistors. The change in resistivity to the third layer at 800 m depth is strong and abrupt, whereas the change between the first and the second layer is generally smooth. The exact depth of this boundary is not clearly defined in the original logs. Only the blocking lets it appear as strong as shown in figure 7.3. The upper 270 m are of medium resistivity of approximately 18 Ω m. The

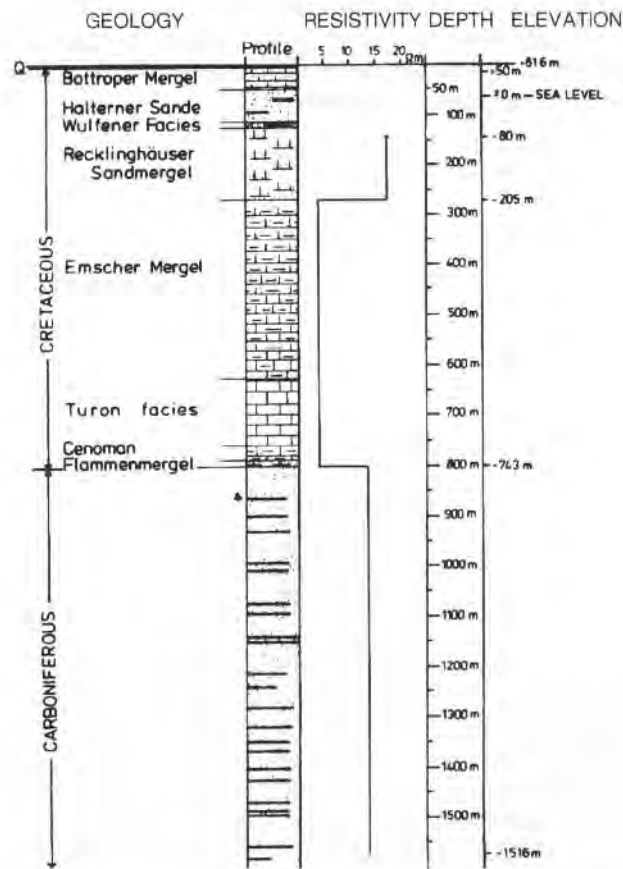


Fig. 7.2: Representative well log derived from borehole measurements within the survey area.

geologic units in this range consist mainly of Marl, sands and limestone of Cretaceous and Quaternary age. Some of the sands in the Haltern Sands are locally water-bearing and thus present problems with reflection seismics. Below this, a conductive unit follows which consists of Marls down to a depth of approximately 1800 m. The resistivity of this unit is approximately 3 Ω m. Below 700 to 800 m, Carboniferous strata has been found with the coal measures in cyclic sequences. In the extreme south of the

LOTEM survey area, two other formations intervene between the Carboniferous and the Cretaceous. These are the upper Permian ("Zechstein") with thin bedded shales, limestones and anhydrites up to 100 m thickness and the lower Triassic ("Buntsandstein") make up of sandstones up to 200 m thickness with high resistivities. The Carboniferous is again of medium resistivity of approximately $15 \Omega\text{m}$. The coarse resistivity model of figure 7.2 was used as a general starting model for the interpretation. This model was then refined using the individual well logs. The resistivities of the well logs were digitized and plotted in the form of cumulative conductance as shown in figure 7.3. These show breaks in their curve when the resistivity boundary changes. The breaks separate the ranges for which linear regression can be used to define the average resistivity for the particular depth range. Generally, this procedure gives very consistent results with the geologic boundaries.

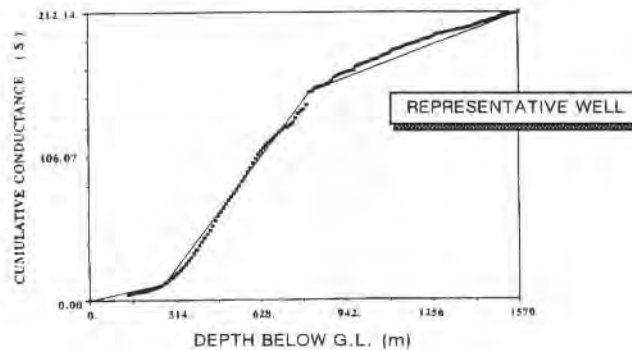


Fig. 7.3: Cumulative conductance analysis to define the resistivity layer boundaries from the well logs (after Stephan et al, 1991).

In figure 7.3 one can observe the smooth resistivity change around the first layer boundary as also indicated by the geology. The change at the second layer boundary is more abrupt. This is best modeled by applying a smooth inversion algorithm (Occam inversion) to the data. The comparison of the Occam inversion with a layered earth well log model can be seen in figure 7.4. Here one can also see a smooth change in resistivity at the first layer boundary whereas the transition to the Carboniferous is more abrupt. The two Occam inversion results were calculated for measurements taken at the same surface location with different receiver systems.

In addition, one seismic section of the area is available for inspection and is displayed in figure 7.5. It is partly interpreted and the thin line is only a general indication for the top of the Carboniferous formation. This section is low data quality and furthermore, the top of Carboniferous formation could not always be detected clearly, i.e. the three strong reflectors indicating the top Carboniferous boundary are not visible at the left and at the extreme right side of this section. This seismic section is mainly used to confirm the horizontal layering of the geological strata and to justify

one-dimensional interpretation for the LOTEM data. More detailed information can be found in Stephan et al (1991).

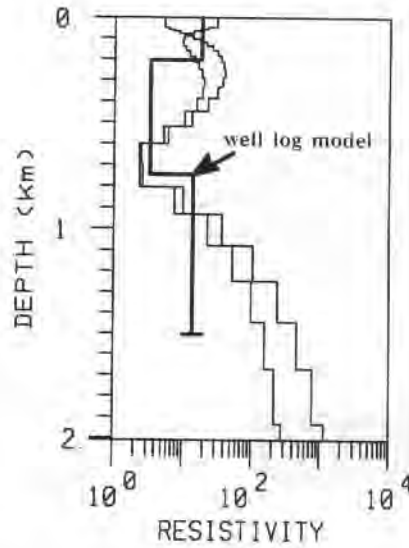


Fig. 7.4: Comparison of two Occam inversion results with a layered earth model.

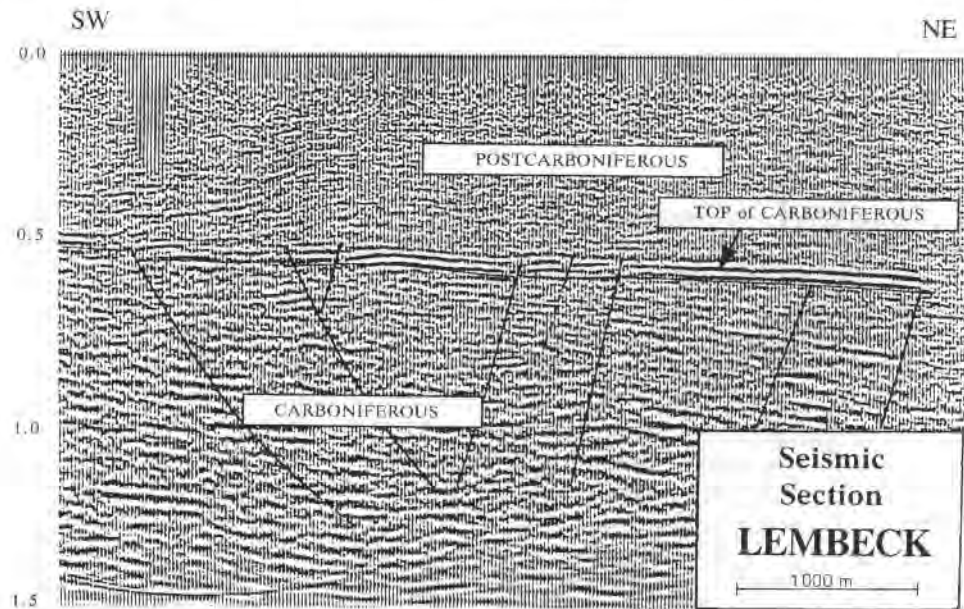


Fig.7.5) Seismic reflection line for the survey area (after Stephan et al, 1991).

The field data in the survey area were extremely noisy. Generally, between 50 to 150 stacks had to be acquired. Figure 7.6 shows the processing steps for two individual records for magnetic and electric field measurements respectively of the 1988 survey. The left column is for the magnetic field and the right one for the electric field measurements. The top row shows the individual raw data. Below, the amplitude spectra are shown which are used strictly for quality control and to design the optimum digital filter. The filtering removes most of the periodic noise in the signal. The bottom row shows the individual records after further smoothing the data with a time variant Hanning window and correcting them for linear drift. The individual records (like the ones shown at the bottom of the figure) are then selectively stacked and yield the signal with much improved signal-to-noise ratio displayed in the top of figure 7.7. At the bottom, the conversion of the data to the logarithmic domain is shown. Here

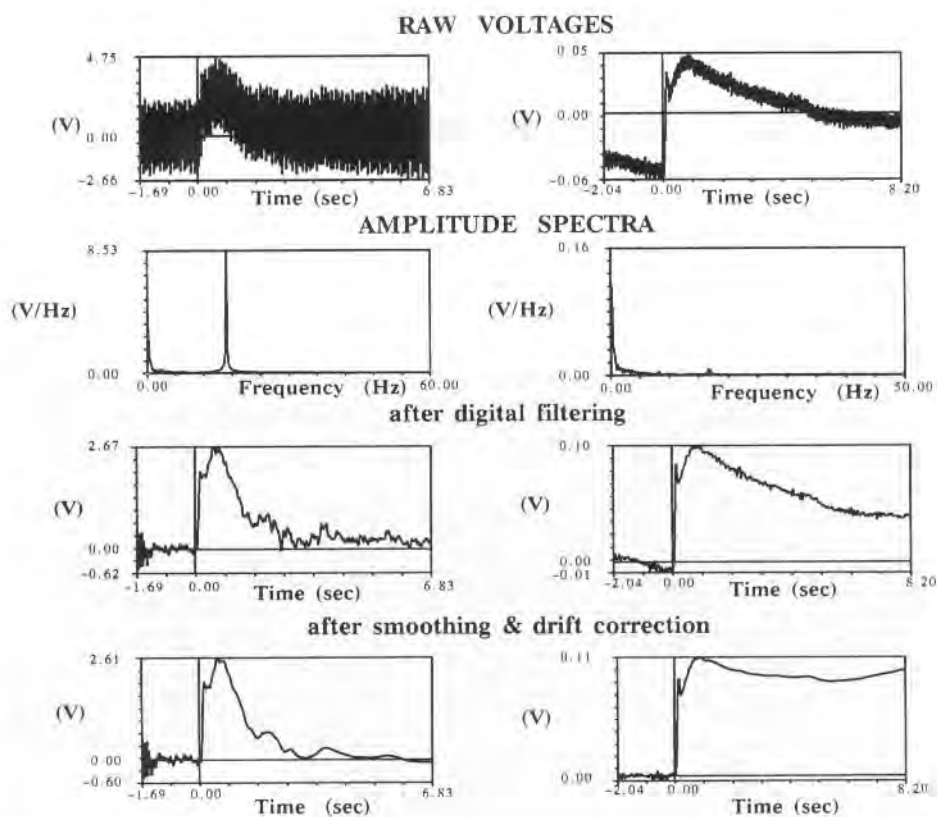


Fig. 7.6: Processing steps for individual raw signals of the magnetic field (left; site A09) and the electric field (right; site B11). The top shows a single record of the raw field data. The second row are the amplitude spectra used for the quality control. Following are the digitally filtered records. At the bottom the further smoothed individual signals are displayed (after Stephan et al, 1991).

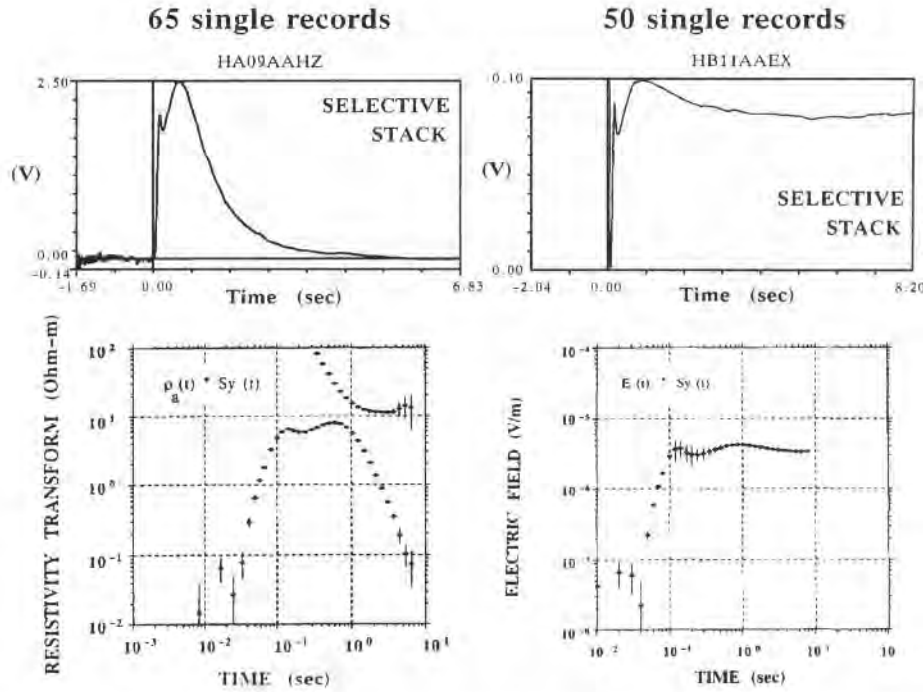


Fig. 7.7: Selectively stacked magnetic field transient from figure 7.5 and the corresponding resistivity transform curve (left). On the right the measured electric field transient is displayed both linearly and logarithmically (after Stephan et al, 1991).

the data are displayed as resistivity transform for the time derivative of the magnetic field, meaning that no corrections for the system response have been applied. The lower curve represents the transformation using the early time apparent resistivity formula and the upper one the transformation using the late time formula. The error bars are derived from the selective stacking algorithm. Figure 7.8 shows the inversion results of this station. The data points representing mainly noise at the beginning and the end of the time series have been edited out. The solid line through the data point represents the theoretical curve derived from the layered earth model on the right. The black dots are derived from the inversion statistics and their radius is proportional to the resolution of the individual parameters. The individual inversion results are then combined to obtain a resistivity cross section as displayed in figure 7.9. This cross section goes through borehole 1 in the South-West and to borehole 2 in the North-East. The inversion results clearly show that the interpretation is very consistent. The error bars in the depth mark the 95% confidence bounds obtained from the inversion statistics. Also, it should be mentioned that the individual model parameters were mostly uncorrelated and no conductance referencing was done.

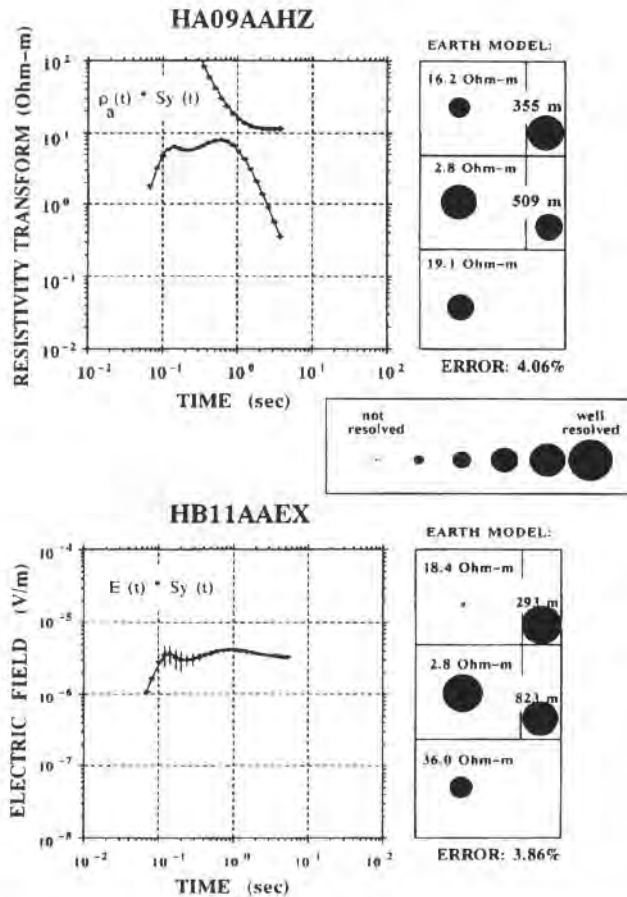


Fig. 7.8: Inversion results of the field data shown in figure 7.6 and figure 7.7 (after Stephan et al., 1991).

Consistency of soundings from different transmitters is a very common problem when carrying out controlled source EM surveys because of possible transmitter overprints (see chapter 4). Two common types of explanations of inconsistencies exist: one caused by inappropriate interpretation of inversion results and the other caused by geologic structure (3-D effect). Before selecting one of the causes and applying corrections through conductance (or transverse resistance) referencing or 3-D modeling as described throughout this book, one must eliminate the stations with data highly contaminated by noise.

The repeatability of the field measurements was checked using measurements from both surveys and all three transmitters. The results are displayed in figure 7.10 for the two sites marked on figure 7.2. In both cases the inversion results are very consistent.

They deviate a little in the resistivity of the last layer. It can be explained that the field data were obtained from magnetic field measurements and magnetic field measurements are not accurate in defining higher resistivities. Furthermore, the measurements at site A were noisier than the measurements at site B. When comparing the measurements of the individual electromagnetic field components (see figure 7.11) it can be seen that they are in general consistent. The deviation in the resistivity of the last layer is now less, since the electric field measurements can more accurately determine the resistivity of this layer (Strack et al, 1989b). At station 17 (right side of figure 7.11) a shift of approximately 50 – 70 m between the well log and the inversion results remains. The cause of this shift is not clearly known, but it could be attributed to a lack of resolution of the LOTEM technique in the upper parts of the section. Because the shift is constant throughout the area, it is not considered to be a significant problem.

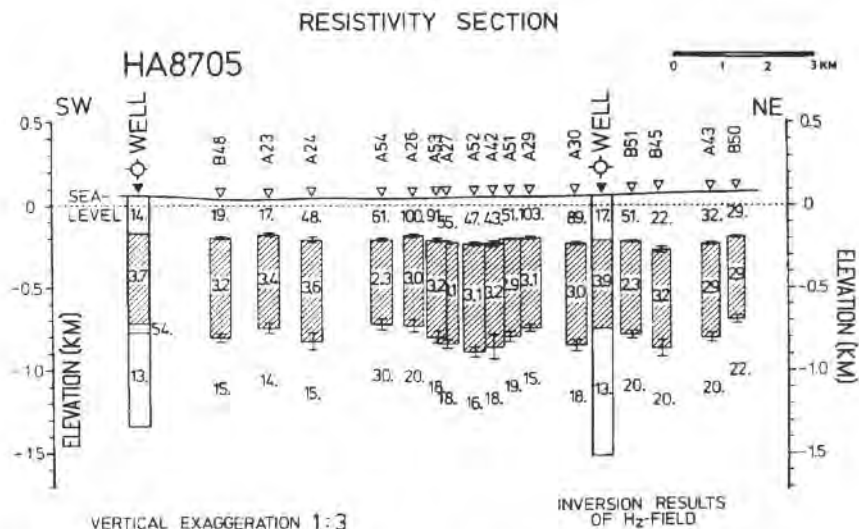


Fig. 7.9: Interpreted resistivity cross section through well nos. 1 and 2 of figure 7.1 (after Stephan et al, 1991).

The large amount of field data requires that the data are first evaluated for consistency of the interpretation. Only when consistency is proven, can general structures within the area be interpreted. One way of showing the consistency is the presentation of the field data in form of contour maps. Figure 7.12 (top) shows a contour map of the resistivity of the conductive unit. Although the inversions were all carried out independently and individually, their resistivity varies little throughout the survey area. The dashed contour lines show the range where the data density was not high enough. This tells us that the interpretation is very consistent throughout the area. No special anomalies exist. To interpret the structure within the survey area, the depth to the *near top of the Carboniferous* was contoured (Near top because in the south-western part of the area it is not clear whether the resistivity contrast is at the top of the Carbonifer-

ous or at the top of the Zechstein);(see figure 7.12). The contour lines are 50 to 70 m deeper (approximately 5 to 8 % of total depth) than expected from the well log but

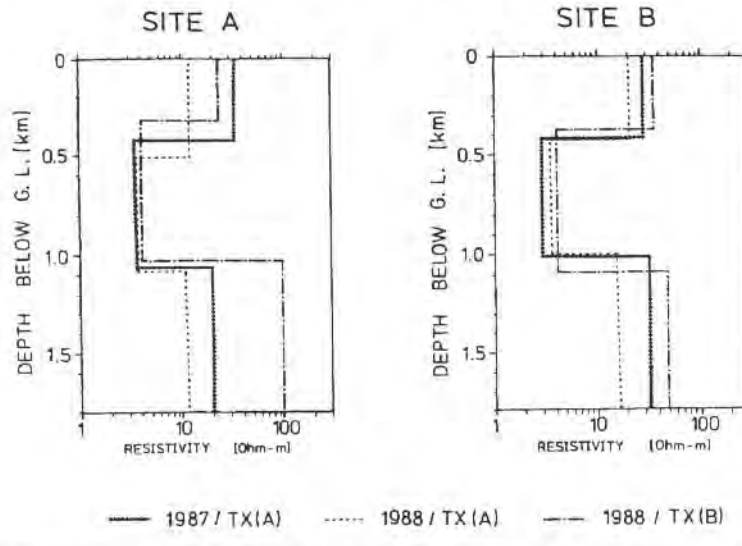


Fig.7.10: Comparison of unconstraint inversion of magnetic field measurements at the same sites using three different transmitters (after Stephan et al, 1991).

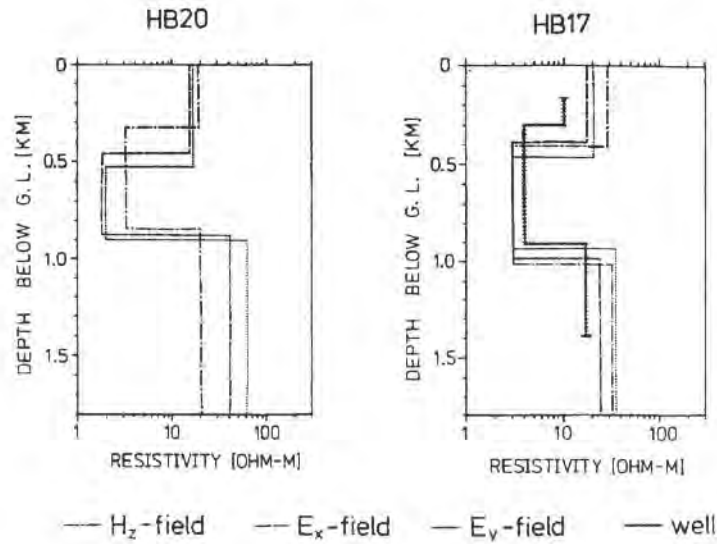


Fig. 7.11: Comparison of inversion of the electric and magnetic field measurements at two sites (after Stephan et al, 1991).

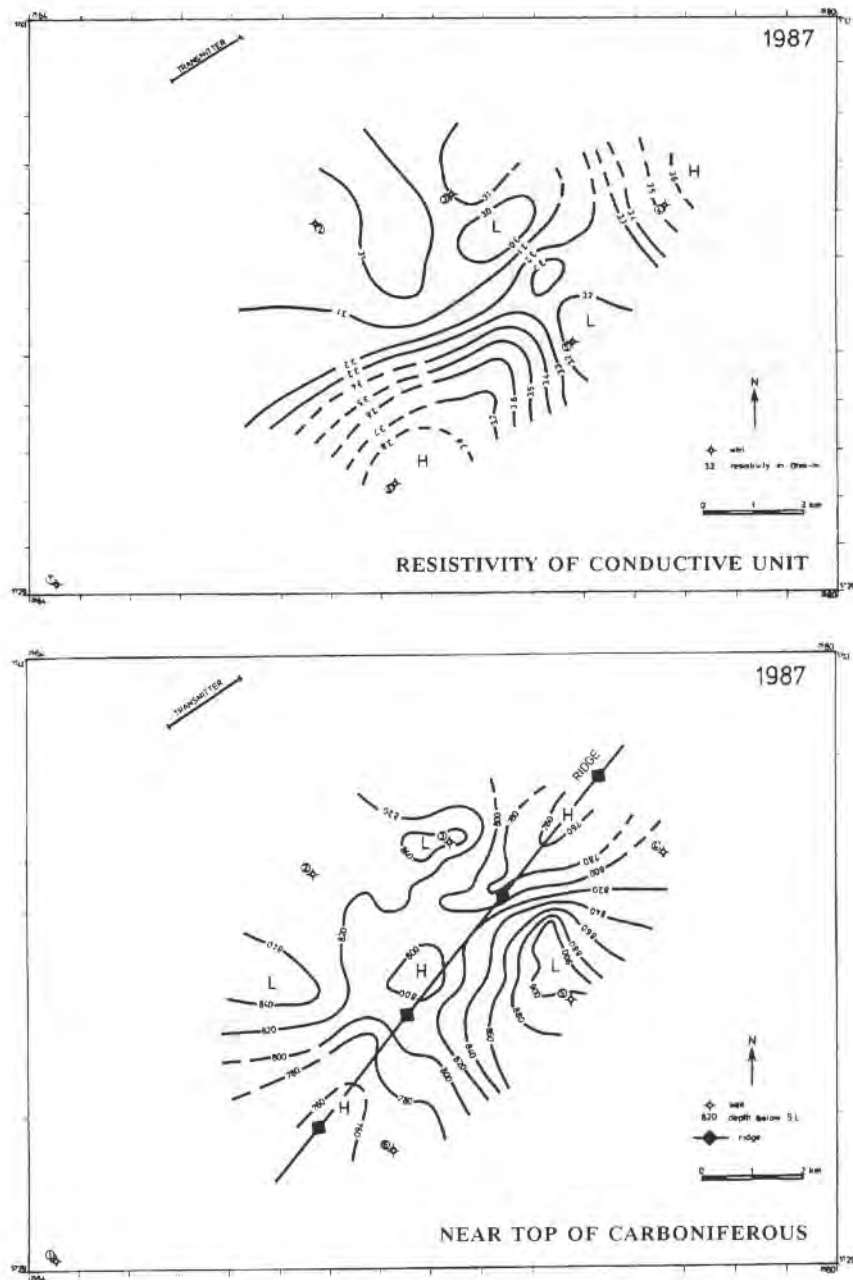


Fig. 7.12: Resistivity contour map of the second conductive layer (top) and contour map showing the near top of Carboniferous (after Stephan et al, 1991).

structurally the results are in accordance with the information obtained from the boreholes. Furthermore, the contours show clearly a ridge which lies between the boreholes and therefore is not indicated directly by the borehole information. This was checked against the geology of the survey area. In figure 7.13 this ridge could be confirmed using a structural map derived from the well known geology of the area.

The above case history shows that the LOTEM survey North of the Ruhr District was very successful. Field data with good signal-to-noise ratio could be obtained even though the field measurements were strongly distorted by cultural noise caused by the nearby industry, power lines and electric railroads. The interpretation yielded results consistent with the well logs. In addition to this, the interpretation showed a ridge in between the well logs which was confirmed by the known geology of the survey area. The field survey allowed clear mapping of the top of the Carboniferous which could not always be obtained from reflection seismic measurements.

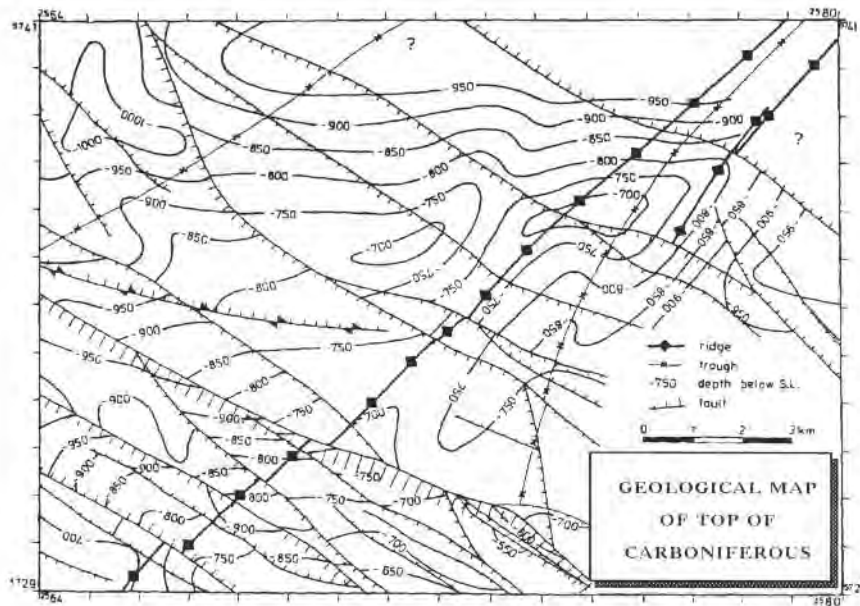


Fig. 7.13: Geologic map for the survey area including the structural interpretation (after Stephan et al., 1991).

GEOLOGICAL CALIBRATION OF THE TECHNIQUE IN THE DENVER-JULESBURG BASIN, USA

An important test with a new technique is to conduct measurements with the instruments over known geology. In the second half of 1981, a test survey was conducted by Group Seven Inc. in the Denver-Julesburg Basin (DJ Basin) with the following objective:

- Calibration of the LOTEM method over known geology.

In order to compare several different receiver systems, the DJ Basin was selected because a great deal of the geology and geoelectric properties is known from the analysis of numerous well logs (Harthill, 1968). This oil-producing basin is located in the north-eastern part of Colorado, USA. The Colorado School of Mines (CSM) test area is shown in figure 7.14. It is approximately 19 kilometers wide and 280 kilometers long. The topography of the area is relatively flat and only minor distortions due to cultural noise (power lines) exist. Within the CSM test area are a number of oil producing fields. Harthill (1968) analyzed several thousand well logs to derive the geoelectric-geologic cross section shown in figure 7.15. The good knowledge of the geoelectric and geologic parameters make this area appropriate for geophysical test measurements.

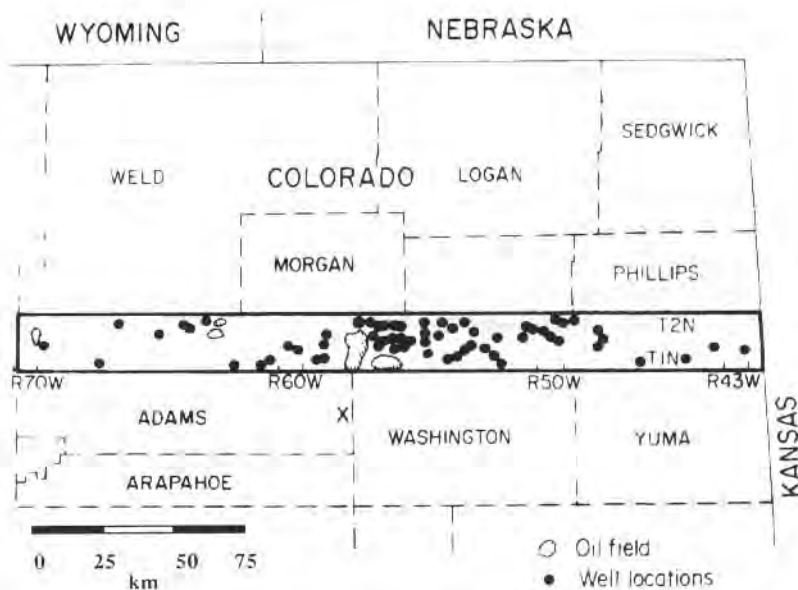


Fig. 7.14) Location map of the Colorado School of Mines test area (heavy border) (after Harthill, 1968).

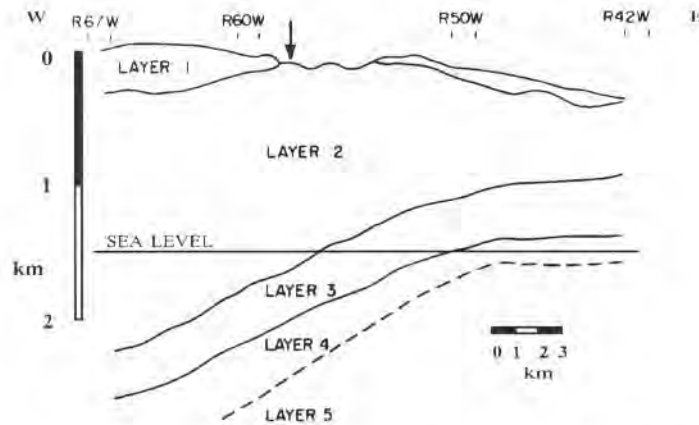


Fig. 7.15: Generalized geoelectric-geologic cross section for the CSM test area (after Harthill, 1968).

The first geologic unit (layer 1) varies through the CSM test area in thickness and resistivity because it consists of a number different geologic formations (Foxhills, Laramie, Denver, Ogallala, Arapaho). Because this layer makes up the weathering layer, the test site was moved 15 kilometers south of the CSM test area (see X in figure 7.14). The test station was located on a crop out of Pierre Shale. The Pierre Shale (layer 2) is geoelectrically fairly homogeneous and has low coefficients of anisotropy (compare figure 1.10). The thickness of the Pierre Shale becomes slightly smaller above the structural high to the east; its resistivity is approximately $3 \Omega\text{m}$. This particular unit has also been of interest for other geophysical test measurements (White et al, 1983; Schneider et al, 1982). The third layer consists of a mixture of sandstones, shales and limestones, and is again electrically uniform (Harthill, 1968). In this layer the Dakota sandstone is highly petroliferous and contains several oil fields in the CSM test area. The thickness of this layer is approximately 400 meters. The longitudinal resistivity for this particular unit is not as constant through the CSM test area as for the Pierre Shale. Also, the anisotropy factor is slightly higher (compare fig. 1.10 for range 58). For an average thickness of 400 meters, the unit's resistivity is approximately $60 \Omega\text{m}$.

The fourth layer consists again of formations which vary in resistivity. However, macroscopically this unit makes up a 300 meter thick layer with high resistivity. The units involved are mainly of Pennsylvanian, Permian and Jurassic ages.

The fifth layer is the precambrian basement consisting of granites and gneisses. Their resistivity is greater than $500 \Omega\text{m}$. Combining layer 4 and 5, one obtains a high resistive unit.

Resulting from this analysis the basic geologic model for the CSM test area is:

Pierre Shale	$\rho_1 = 3 \Omega\text{m}$	$H_1 = 1600 \text{ m}$
Sandstones	$\rho_2 = 6 \Omega\text{m}$	$H_2 = 1600 \text{ m}$
Electrical basement	$\rho_3 = 500 \Omega\text{m}$	

The field system consisted of three of Group Seven's receiver systems. All of the systems used SQUID magnetometers as receivers. All SQUIDS were different models of different age. One of the biggest problems with the receiver systems was the instability of the superconducting magnetometers and lengthy system calibrations had to be done with all systems to obtain comparable results. The apparent resistivity curves for three different receiver systems are shown in figure 7.16. Even after careful system calibrations the system responses of the three different systems are sufficiently different that deconvolution could not restore the signals to become close to each other earlier than 300 milliseconds. Also, at later times, high frequency noise can be seen. However, it is remarkable that in the intermediate time range the apparent resistivity curves for all three systems are almost identical. Thus the data points before 300 milliseconds were eliminated and at later times smoothed yielding a reliable estimate for the sounding at the test station and eliminating the noise of the RF amplifiers of the SQUIDS. As transmitter, a 1.5 kilometer grounded dipole was used at 15 kilometers distance north of the receiver site.

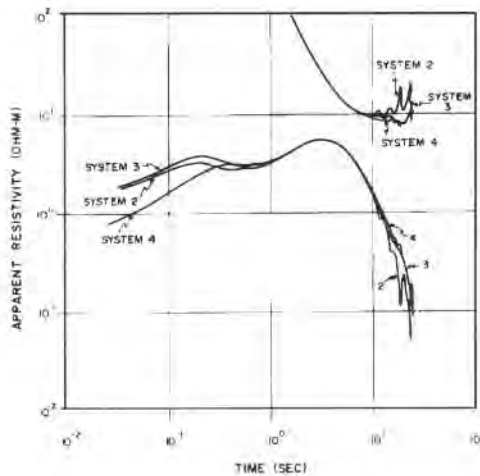


Fig. 7.16: Apparent resistivity curves for the LOTEM measurements over the CSM test area (after Strack, 1985).

The deconvolved smoothed apparent resistivity curves were then compared with the synthetic curves for the geoelectric model published by Harthill (1968). The result of this comparison is displayed in figure 7.17. The match between the field data (dots) and the synthetic curve (solid line) is quite good and thus the geologic calibration of

the systems was successful. From these test measurements further improvements in the data handling procedures and instruments were then derived.

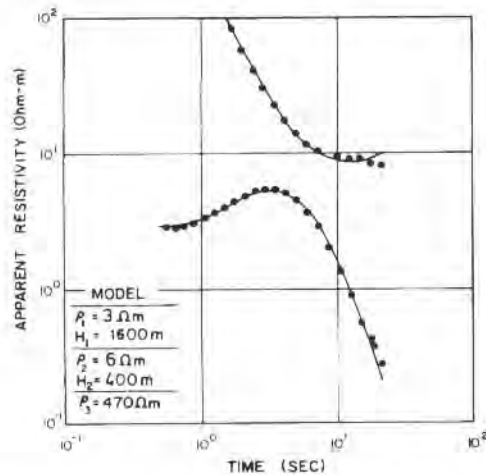


Fig. 7.17: LOTEM field data (dots) and theoretical curves (solid line) for the generalized geoelectric model in figure 7.15 (after Strack, 1985).

FIRST FIELD TESTS IN AUSTRALIA (SYDNEY BASIN)

During 1983 a prototype LOTEM system (DEMS III) was built at Macquarie University and tested in the Sydney Basin. The objectives of the test measurements were twofold:

- Demonstration that the LOTEM method can be applied in difficult areas such as the densely populated Sydney Basin near Sydney. Also the resistivity structure was to be determined for a depth range of 1 to 4 kilometers.
- Demonstration of the simple operation of the entire field system, including data processing, giving special attention to the cost.

The research was funded by a Macquarie University research grant supporting the collaboration between CSIRO, Macquarie University and BHP. A summary of the measurements can be found in Strack (1984).

The measurements were conducted during two days during October, 1983, in an area located about 20 kilometers north-west of Sydney. The Sydney Basin is approximately 380 kilometers long with a total continental area of 36,000 squarekilometres and lies along the east coast of New South Wales (see figure 7.18). The Sydney Basin is divided into five areas: the Southern Area, the Western Area, the Central Area, the Northern Area, and the North-Western Area. In all areas coal is/has been produced.

The individual areas are further subdivided into sub-basins. Hydrocarbons have been found in the Sydney Basin but not in commercial quantities. The test area was selected due to its closeness and accessibility with respect to Sydney and the fact that a topographic map showed the area as open for the receiver sites, and transmitter setup seemed possible in the creeks. When the measurements were being conducted, only a limited number of clearings could be found which explains the distribution of the receiver sites shown in figure 7.19.

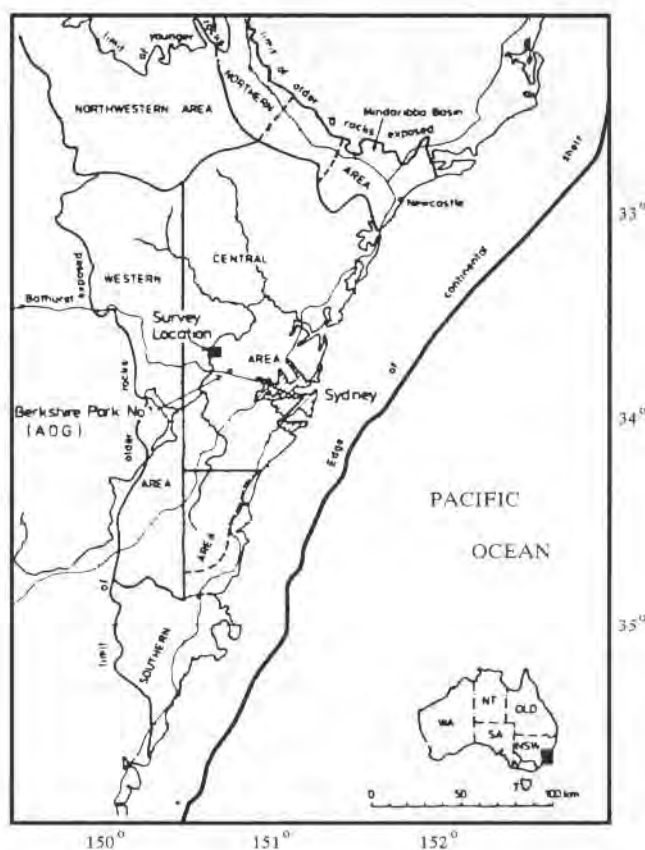


Fig. 7.18: Generalized geographic location map of the LOTEM survey area in the Sydney Basin (after Strack, 1984).

The geology of the Sydney Basin consists of a complex mixture of deltaic and marine sediments which results potentially in mainly stratigraphic hydrocarbon traps. This makes the interpretation of geophysical data more complicated because detailed borehole control is required. A more detailed description of the geology of the Sydney Basin can be found in Mayne et al (1974). Figure 7.20 shows a simplified geological cross-section in north-south direction through the Sydney Basin. The arrow marks the

approximate location of the survey area. At this location the strata are horizontally layered (conformably) to a depth of about 3 kilometers, and resistivity contrasts due to lithology are expected. From this section an approximate inversion starting model was postulated. A newer east-west section is shown in figure 7.21 (Mayne et al, 1974), which gives a better overview of the lithology of the Sydney Basin. The exact depth of the Sydney Basin is yet not known.

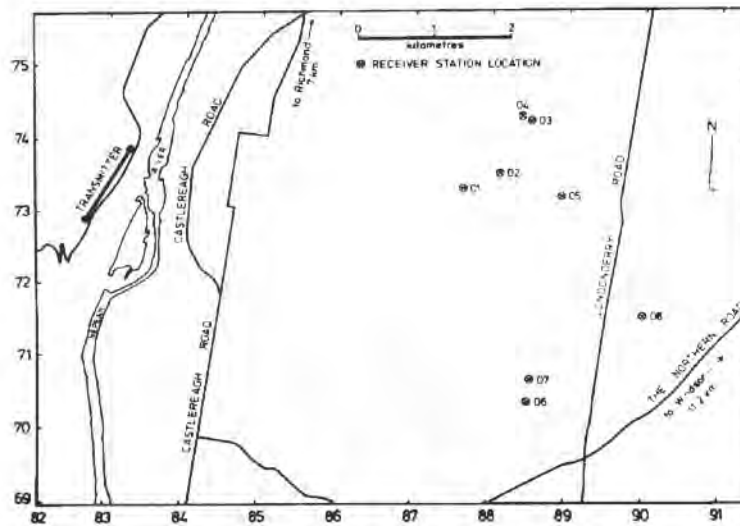


Fig. 7.19: Survey plan of the LOTEM receiver and transmitter sites (after Strack, 1984).

At 8 receiver sites approximately 320 individual transients were recorded. Due to the strong thunderstorm activity during the field days the actual recording time was less than 8 hours. The rest of the time was used for the setup and breakdown of the transmitter. The transmitter dipole was 1200 m long and the electrodes were implanted in the bed of two creeks. The creek beds contain little mud and thus only a current of up to 45 amperes could be injected into the ground. As receiver, a standard 200 m long seismic cable with about 100 conductors was used as induction coil. Figure 7.22 shows the selectively stacked LOTEM transients at all receiver sites. The data become increasingly noisy going towards station 8 because of thunderstorm activity and thus the electromagnetic noise was increasing with time. No data processing was done prestack, which could be part of the reason why the stack of station 8 is so noisy. After stacking the data were filtered, smoothed and the system response deconvolved. An example of the resulting apparent resistivity curves is shown in figure 7.23. The apparent resistivity curve shows already three distinctive layers at early times (compare flexure in figure 7.23).

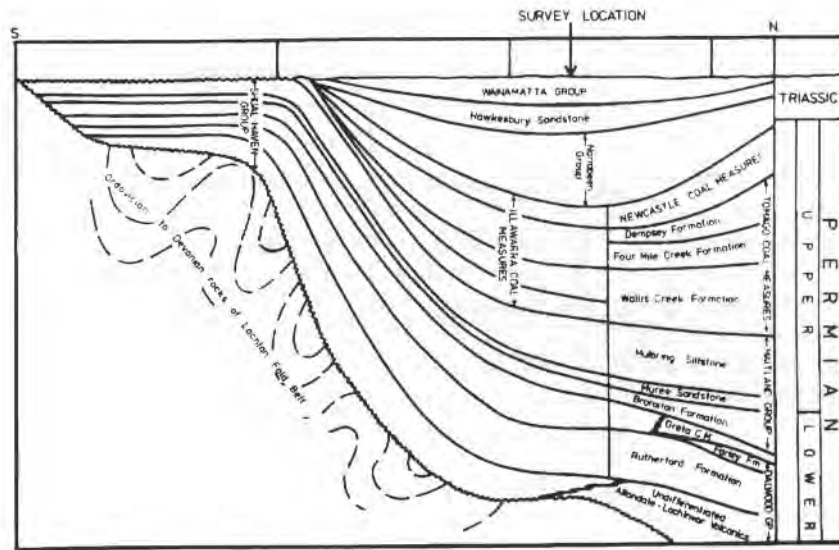


Fig. 7.20: Simplified general geological north-south cross section of the Sydney Basin (after Strack, 1984).

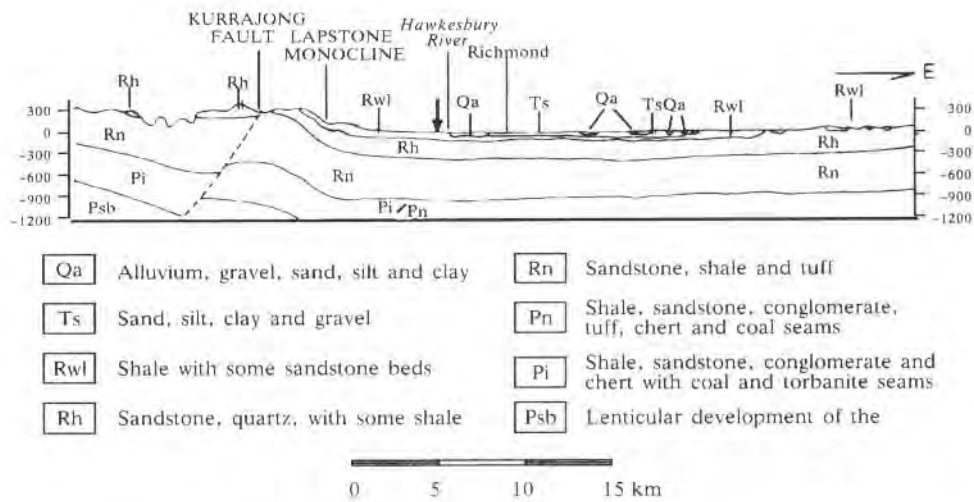


Fig. 7.21: Simplified shallow geologic west-east cross section of the Sydney Basin (after Strack, 1985).

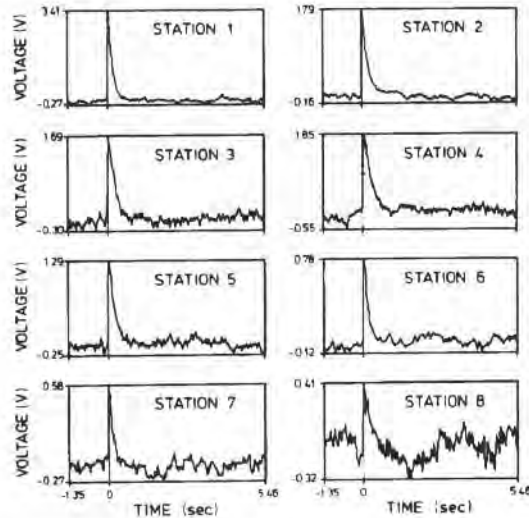


Fig. 7.22: Selectively stacked LOTEM transients of the eight receiver sites (after Strack, 1984).

The known geology required a three-layer starting model. After inversion tests it was found that the inversion required an additional fourth conductive layer which could not be explained initially. Later on this conductive layer was explained by the geology.

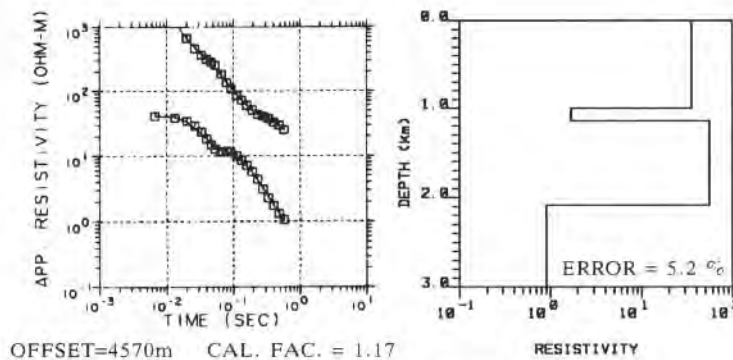


Fig.7.23: Inversion result for receiver site 1 (after Strack, 1985).

The first layer in the starting model consists of a mixture of sandstones, shales, conglomerates and tuffs, the second of a sequence of sandstones, clay shales, tuffs, oil shales and coals. In general one would expect the resistivity of this layer to be the same as the resistivity of the first layer. However, the inversion clearly required this layer to be more conductive. Later on, the analysis of the well completion report showed that the clays in this layer are responsible for the high conductivity of it. The

third layer consisted again of sandstones and shales with a slightly higher resistivity than the first layer. The only information on the fourth layer is that it probably correlates with the Greta coal measures. The geoelectric parameters of the first layer are well resolved, whereas for the second layer only the conductance is resolved. For the third layer the total thickness to the conductor below is resolved, but the resistivity of the third layer not.

Figure 7.24 shows the interpreted geologic cross-section in comparison with the results from the BMR bulletin 149 (Mayne et al, 1974). The fourth layer consists of approximately 1 kilometer sediments of Triassic to Permian age. The base of this layer lies (from the LOTEM measurements) at approximately 1 kilometer depth. The seismic results give the base of the Narrabeen Group at 850 meters. Analysis of several well completion reports says that the late Permian coal measures below start quite sandy at the base of the of the Narrabeen Group. This explains why the conductivity contrast is below the seismic reflector. The second layer correlates with late Permian

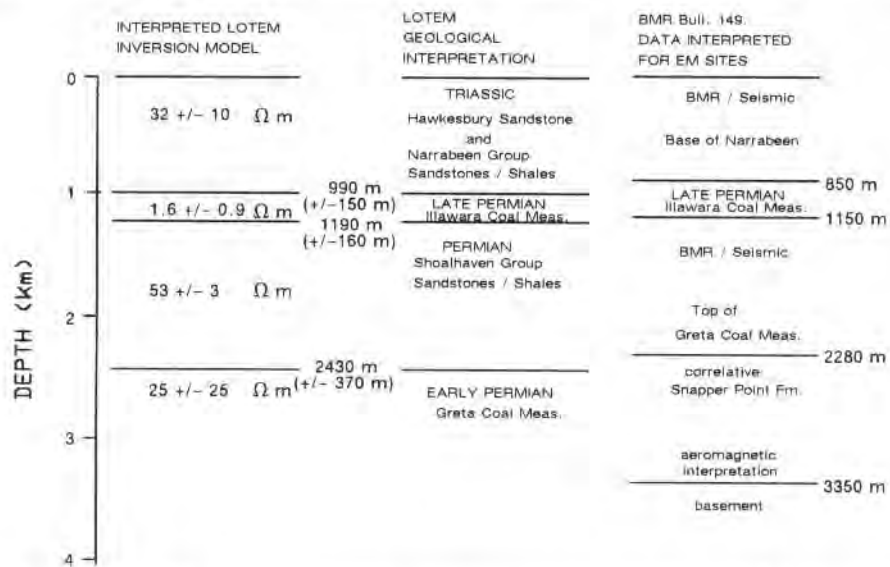


Fig.7.24: Interpreted geological section in comparison with the results from BMR bulletin 149 (after Strack, 1984).

Illawarra coal measures which are in general more resistive. This layer, however, is seen by the LOTEM method as very conductive because of the clay beds within it. The base of the coal measures is in the LOTEM interpretation at approximately 1200 m with 1150 m from the seismic interpretation. The correlation of this horizon is probably caused by abrupt facies changes between the late Permian coal measures and the Shoalhaven Group below. The third layer is a 1200 meter thick unit of resistive marine sequences interpreted to be of the Permian Shoalhaven Group. The average geoelectric boundary at 2430 meters depth is thought to correlate with the seismic pick

at the top of the Greta coal measures and the correlative Snapper point formation at 2280 meters. The discrepancy in the interpretation between the LOTEM and the seismic could either be caused by the LOTEM or the seismic which is based on unmigrated data.

Figure 7.25 shows a comparison of the LOTEM interpretation with the interpretation of audio magnetotelluric data, SIROTEM data and UTEM data. The results of two well logs within the vicinity of the area are also shown. Unfortunately, the wells are too far away from the survey area thus only a qualitative correlation can be done. The Kurrajong Heights (not shown) well shows a very good conductor around 1 kilometer

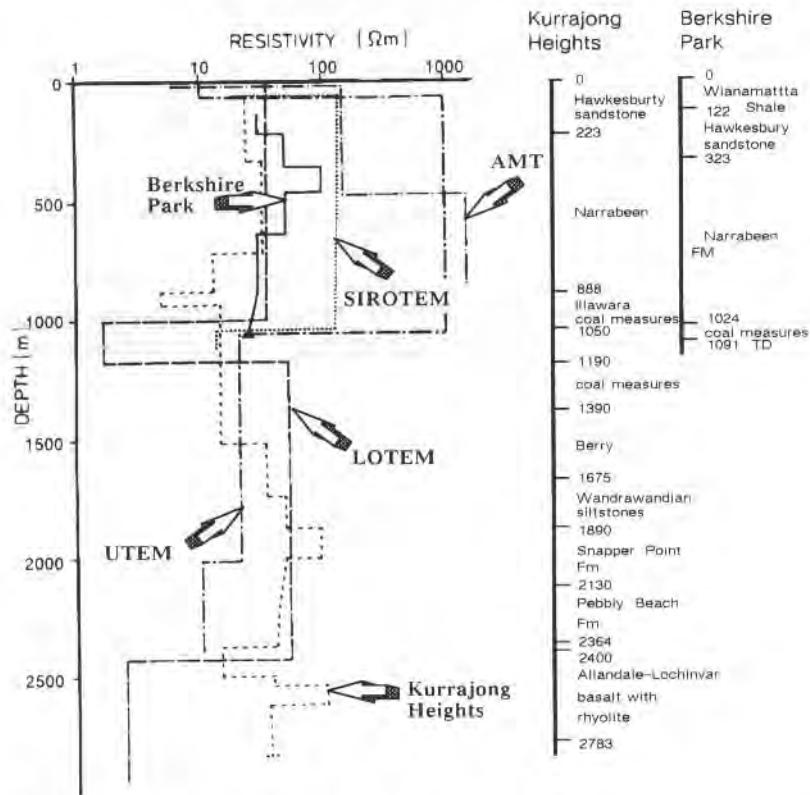


Fig. 7.25: Comparison of inversion results with other geophysical techniques and well log data (modified after Vozoff et al, 1984).

depth. The other well, the Berkshire Park, only goes to approximately 1100 meters depth and does not penetrate this conductive unit. However, this well also shows a decreased in resistivity around 1 kilometer depth. The audio magnetotelluric (AMT) measurements do not penetrate deeper than 500 meters due to the noise in the area. The SIROTEM data shows also a very strong resistivity change towards more conduc-

tive units at approximately the same depth as the LOTEM. However, the resistivities of the SIROTEM measurements are approximately three times larger than the LOTEM measurements. This can either be attributed to the different coupling of the transmitter (the LOTEM uses an earthed dipole, whereas the SIROTEM system uses an induction loop) or systematic differences in the interpretation procedures between both systems. The UTEM results are higher in the upper kilometer as are these of the LOTEM and SIROTEM but very closely approach the SIROTEM resistivity values around 1 kilometer depth. In general the LOTEM measurements average the resistivity of the two wells in the upper kilometer nicely. The LOTEM resistivity seems to be fairly close to the average resistivity for the well log. Since inductive source systems do not resolve resistors as well as galvanic source systems (see chapter 8), the derivation in the resistivity of the SIROTEM and UTEM data from the LOTEM data and well log is acceptable.

The above case history demonstrates that the LOTEM technique could be successfully applied to new exploration problems with a fairly simple prototype system. The data interpretation was done quite rapidly and the interpretation results are comparable with the additional geophysical information available from the survey area.

3-D INTERPRETATION CASE HISTORY MÜNSTERLAND BASIN, FRG

During 1987, a field survey was carried out in the Münsterland Basin near the 5 km deep borehole Münsterland 1. The objective of the survey was to calibrate the method in an area of known geology. Some parts of the survey area show anomalous transients which indicate a 3-D structure. Here, focus is given on the interpretation of these anomalous transients as described by Hördt et al (1991).

Figure 7.26 shows the distribution of the LOTEM stations in the survey area. Magnetotellurics (MT) and Controlled Source Audio-frequency Magnetotellurics (CSAMT) data were recorded in this area at an earlier date by other research groups. They were used for comparison with the results of the LOTEM survey and for 1-D joint inversion with the LOTEM data (Hördt et al, 1991). The LOTEM stations lie along two profiles, which cross near the location of the borehole Münsterland 1. The shaded area denotes the region where 3-D effects were observed in the data. The creeks are related to the geology and are shown in figure 7.26 for orientation.

Figure 7.27 shows the results of 1-D inversions along the profile ML8701, using a second order Marquardt algorithm (Jupp and Vozoff, 1975). To improve the consistency along the profile, the final model of one station serves as the initial model for the next, starting from the western end. The section shows a consistent three-layer model in the western part of the area, but is different in the eastern part (the shaded area in figure 7.25). Stations A03, A07 and A06 require a first layer which is more resistive and thicker than on the rest of the profile.

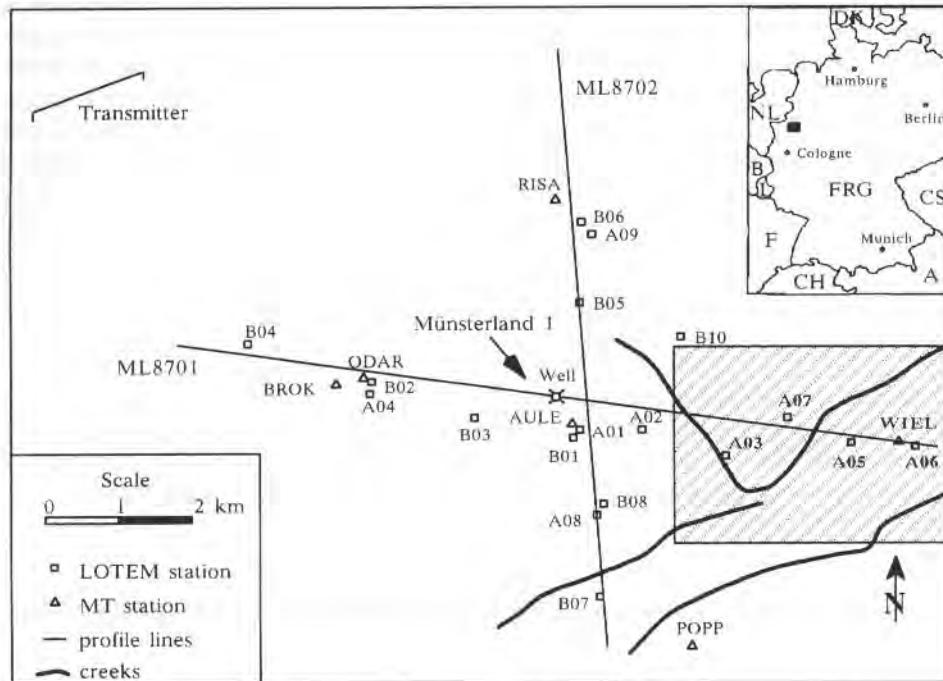


Fig. 7.26: Basemap showing the LOTEM and MT stations in the Münsterland survey area. The shaded area denotes the 3-D region. The creeks are indicated for orientation.

Also displayed in figure 7.27 are six selected data sets. (The field data still contain the system response and look different from synthetic 1-D data at early times. For numerical stability the forward modeling curves are convolved with the measured system response of the corresponding data set, rather than carrying out the deconvolution.) Stations B03 and A01 belong to the consistent part of the profile and show the typical curve shape for this survey area. Stations A03, A07 and A06 have a larger amplitude at early times. A satisfactory fit could be obtained with 1-D inversion, but in fact the large early-time amplitude is a 3-D effect. Station A05 includes a sign reversal in the measured voltage curve which cannot occur over a layered half-space (Newman, 1989). Thus, this station cannot be interpreted using 1-D inversion and clearly indicates a 3-D structure.

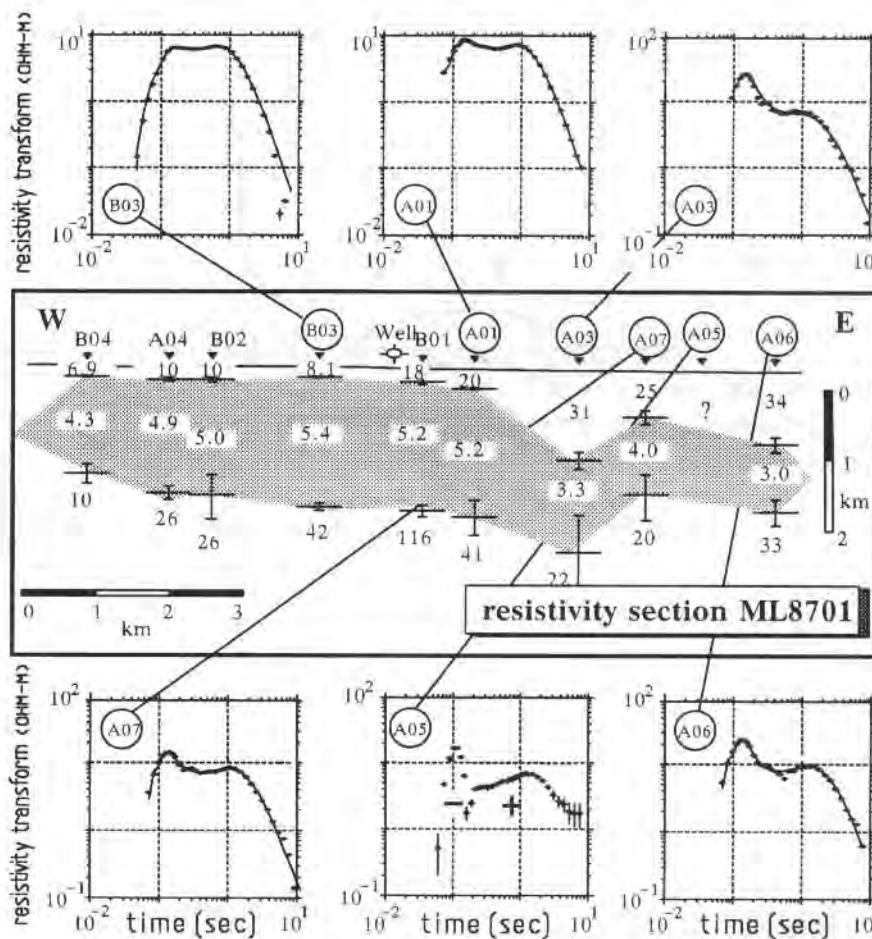


Fig. 7.27: Inversion results along profile ML8701 with the data sets around the 3-D anomaly. The squares correspond to the measured, the solid lines to the calculated data. Data sets B03 and A01 show layered behavior, the other data sets show 3-D effects. Station A05 includes a sign reversal on a linear scale. On the logarithmic scale in the figure the absolute values are shown. The positive and negative data for site A05 are indicated by "+" and "-".

Newman (1989) explains that a near-surface conductor causes a sign reversal if the station is on the side away from the transmitter. On the side towards the transmitter the curve is shifted to higher amplitudes at early times. This effect can be observed in the model responses, used for comparison of the 3-D programs (compare chapter 4). A sketch of a simplified physical explanation is presented in figure 7.28. After the transmitter current is switched, the induced currents in the earth are channelled through the conductive body. This causes a local anomalous current and associated anomalous magnetic field. At the receiver sites towards the transmitter this anomalous

magnetic increases the total magnetic field; beyond the anomaly the total magnetic field is reduced, and possibly causing a sign reversal. The lower part of the figure shows the calculated 3-D responses along the profile over the body for 10, 50 and 100 ms after the current switching. The dipole-type response of the conductor is visible for early times.

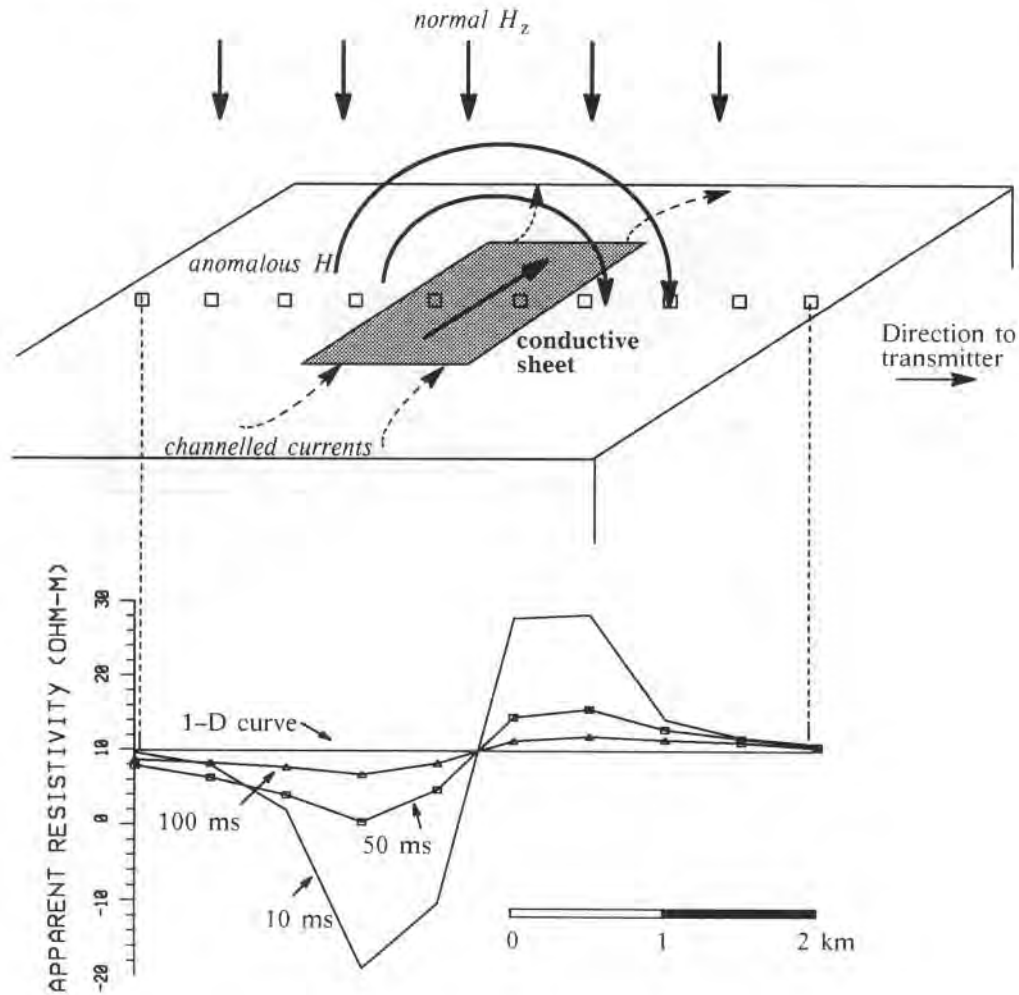


Fig. 7.28: Physical explanation of the 3-D effects observed in the field data. The upper part of the figure schematically shows the behaviour of currents and magnetic fields when the 1-D structure is disturbed by a local conductive body. The squares are the receiver locations on the surface. The lower part shows the apparent resistivity for different times along the profile over the body in comparison with the 1-D response.

Results of Thin-Sheet Modeling

After explaining the observed 3-D response, we apply the 3-D forward modeling routines to obtain a quantitative interpretation. First, we select a conductive body with one edge somewhere between stations A07 and A03 and another between A07 and A05 (figure 7.29). This model will not explain the data set A06, which shows similar behaviour as A03 and A07, because site A06 is on the wrong side of the anomaly. To explain the measurements at station A06 one would have to construct a model with an additional body. At this stage there are not sufficient geological information or LOTEM data to interpret station A06 at the end of the profile. We will thus concentrate on finding a quantitative explanation of the three stations A03, A07 and A05. The data set A06 will be discussed at the end of the paper.

Even with the above starting model it is still a cumbersome trial-and-error procedure to find a thin-sheet model which fits the data. Thus, we incorporated the thin-sheet modeling into an inversion routine, using an algorithm for the 1-D inversions (Jupp and Vozoff, 1975). The variable parameters are the conductance of the thin sheet and its depth. All other parameters, such as strike, position and horizontal extensions of the sheet are fixed. The underlying 1-D earth is also kept fixed at the parameters of the nearest non-3-D station A01. This incorporates the reasonable assumption that in the 3-D area the layering does not change, but is disturbed by a local structure.

Some forward modeling was necessary to find a reasonable starting model. For the first model runs, the 3-D effect on the calculated data was not large enough. The reversal occurred at very early times and was not comparable with the large effect in the data of station A05. We found that we had to use an elongated sheet with strike approximately SW-NE and with increased conductance. Different models which appeared promising after the forward modeling were used as starting models for the inversions. Figure 7.29 shows the best-fitting thin-sheet model, with the corresponding data fits illustrated in figure 7.30. Considering the simplicity of the model, the fits are extremely good. Note also that the early-time amplitudes of station A03 and A07 are well-matched. This was a difficult task because the 3-D effect at station A03 is larger than at station A07, although site A07 is closer to the expected position of the anomalous structure. For the model in figure 7.29 station A07 is so close to the midpoint of the sheet that the 3-D effect is weaker than at station A03. Figure 7.28 illustrates how the 3-D effect becomes smaller when approaching the midpoint of the anomaly, because the scattered magnetic field becomes predominantly horizontal.

The drawback of the model in figure 7.29 lies in the shallow depth of the thin-sheet and its high conductance. This was a common feature of all inversion results. The inversion always moved the sheet towards the surface and increased the conductance, suggesting a man-made conductor – such as railroad tracks or power lines – as cause of the anomaly (Sternberg, 1979). Since these do not exist in this area, we assume that

the shallow depth and the high conductance are an effect of the thin-sheet modeling. The true conductivity structure is probably much more complicated than a thin sheet, and the conductive anomaly could extend vertically rather than horizontally. Thus, we cannot expect to determine the correct depth to the anomalous zone. We can conclude from the thin-sheet modeling that we can fit the data with a conductive anomaly between station A03, A07, and A05, and that the strike is approximately SW-NE. With this information we refine our model further using another 3-D program.

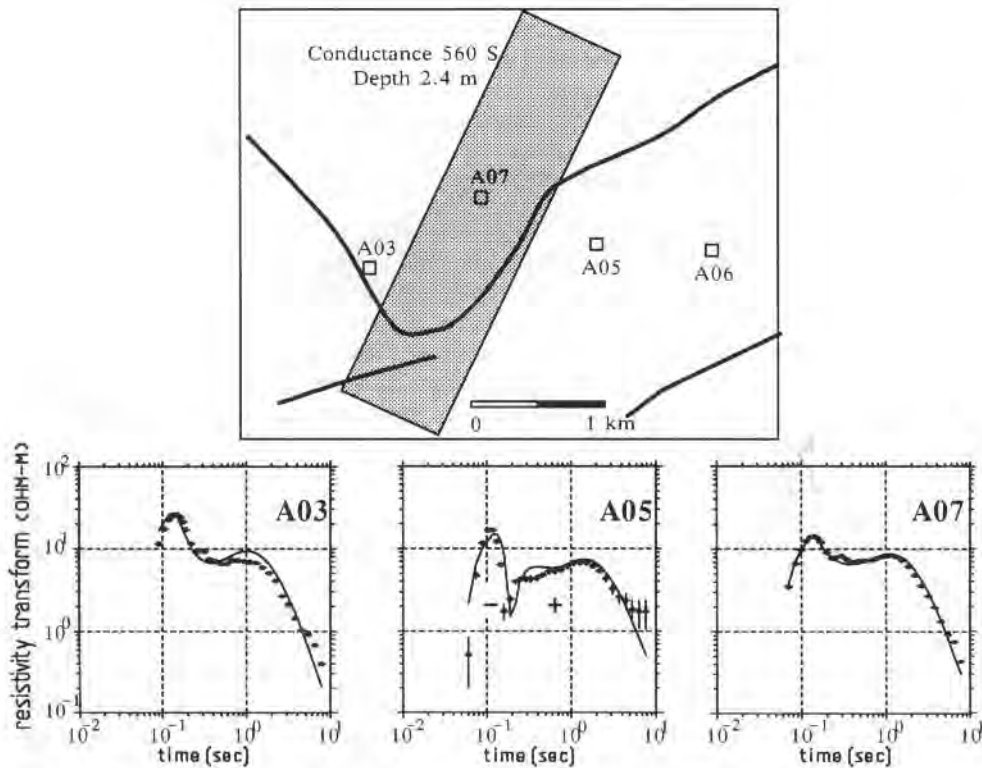


Fig. 7.29: The "best fit" thin-sheet inversion model (plan view). The map corresponds to the shaded area in figure 7.26.

Results of Integral Equation Modeling

After the thin-sheet modeling we must incorporate the geology as a priori information to reduce the number of possible models. The survey area lies within a large sedimentary basin with the upper 1500 m consisting of Cretaceous North Sea Basin deposits. Geoelectrically, the area is horizontally layered. There are no indications of large conductivity anomalies in the upper few hundred metres (Jödicke, 1990). The

only reasonable explanation of the anomaly is deep brine, which is very conductive and could move to the surface along faults or weak zones.

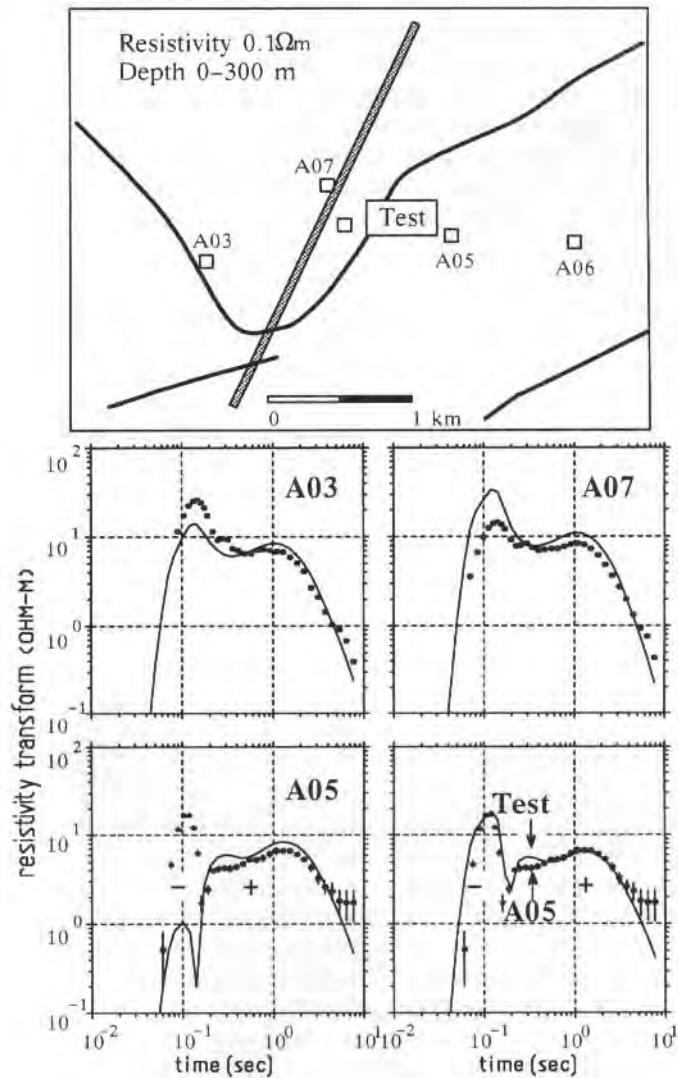


Fig. 7.30: The 3-D model (plan view) used for the simulation with the IE program. The midpoint and the strike of the conductive body are the same as for the thin-sheet model in figure 7.29. The body extends from the surface down to 300 m depth. Data fit for the model configuration is displayed at the bottom. The squares correspond to the measured data, the solid line is the calculated curve. The bottom shows a comparison of data set A05 with the calculated curve of location "Test". It gives a better fit than the calculated curve at the location of site A05.

We constructed a model based on the best fit of the thin-sheet inversion, but considering the possible mechanism for the resistivity decrease. A plan view of the model is shown in figure 7.30. The strike of the anomalous structure is the same as for the thin-sheet model in figure 7.29 with 50 m width and 300 m depth extent. This simulates a shear zone where the brine rises and decreases the resistivity. From the geology we expect this zone to be approximately 100 m wide close to the surface and only approximately 10 m thick at 50 m depth. Moreover, it would not be vertical, but rather would dip at an angle of approximately 60 degrees (Staude, 1990, pers. comm.). However, we want to keep our model as simple as possible, simulating only structures which can be resolved with the LOTEM method. Due to the sparse distribution of stations in the area we can only justify a model with a simple body of vertical extent. Figure 7.30 shows the data fits for this model. The fits are worse than the thin-sheet modeling results (compare figure 7.29). The early time amplitudes do not match for stations A03 and A07, and the reversal effect is too small for station A05. This suggests that for a vertical structure the receiver must be close to the anomaly to get strong effects. To test this assumption, the field data of station A05 is compared with the calculated data (see figure 7.30) of a fictitious station marked "Test" in figure 7.30. This location is only 200 m away from the anomaly, whereas the A05 location is 900 m away. The "Test" curve is very similar to the field data, indicating that for near-surface anomalous zones a vertically extended body gives a spatially narrower effect than a body of horizontal extent. In the next phase of interpretation we must construct a model where stations A03 and A05 are closer to the anomalous body.

Results of SLDM Modeling

The modeling results given above suggest a modification of the position and possibly the strike direction of the conductive body. We now construct a model, where stations A03 and A05 are closer to the anomaly, because the 3-D effect in the respective data is strong. Station A07 must be farther away from the body, because the 3-D effect is weaker there. There are some mapped faults in the area; one of them crosses at station A03. The strike of the fault is SE-NW, and not, as we expect from the above modeling, SW-NE. The creeks in the area correspond to the geology. They flow along former weak zones, and from a geological surface map the branch flowing in SE direction is almost coincident with a known fault (Staude, 1989). The resultant model, where the conductive structure correlates with the creeks and mapped faults at the surface is shown in figure 7.29. It consists of two plates, one striking SW-NE, and the other one striking SE-NW. This is a very difficult task for the integral equation program, but it is a reasonable model for the SLDM program, which has been designed for large structures like this.

The results of the forward modeling are shown in figure 7.32. The data fit is very good for stations A03 and A05. Note that now the early time part of A03 is fit nicely by the modeled curve. The fit is not perfect for station A07. One could improve the model further to reduce the deviation for A07. This requires additional model runs

where we modify our model step by step. Initial testing has shown that the main conclusions do not change substantially in this process.

The SLDM model

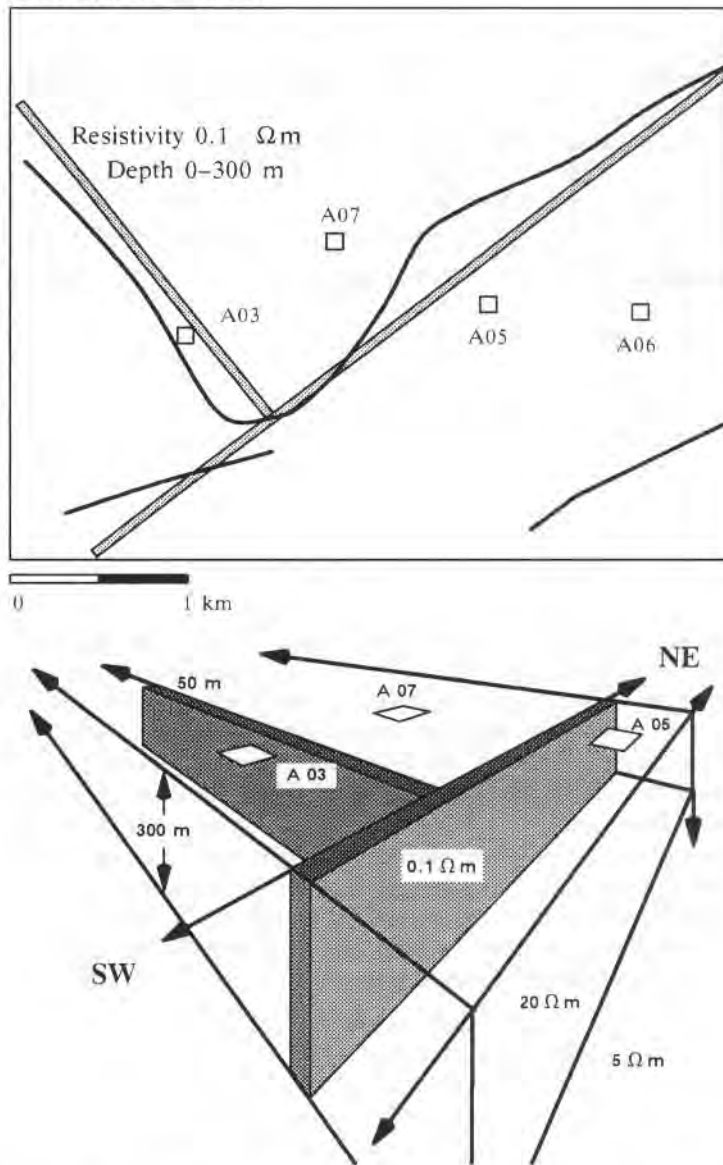


Fig. 7.31: Top: The 3-D model (plan view) used for the simulation with the SLDM program. Bottom: Schematic 3-D sketch of the 3-D SLDM model (after Hördt et al, 1992).

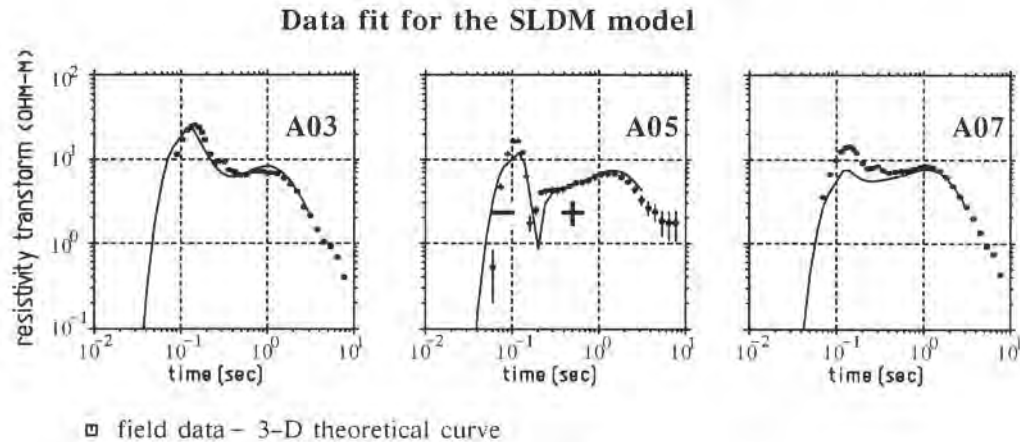


Fig. 7.32: Data fit for the SLDM simulation. The squares correspond to the measured data, the solid line is the calculated curve (after Hördt et al, 1992).

Discussion of 3-D Interpretation

In three steps we derived a 3-D earth model which fits our observed LOTEM data and also corresponds to the geology. In the first step we determined the approximate position and the strike of the anomalous structure with a thin-sheet inversion routine. In the second step we calculated the response for a more complex model which integrates a possible geological cause of the 3-D effects using an integral equation program. This showed that we had to modify the strike of the structure, because the now vertically extended body causes a spatially narrower anomaly than a horizontal thin sheet. In the last step we derived a realistic model – which is too complex for calculation with the integral equation program – applying a finite-difference algorithm (SLDM). The model was constructed with the outcrop of the bodies being below creeks at the surface. The geological explanation is deep brine rising along weak zones (Staude, 1989) which causes the decrease in resistivity.

The correlation between the interpretation and the geology is very good, with some open questions remaining. The data of station A06, which also shows a 3-D effect, cannot be explained by any of our models. We assume that this data is influenced by a different structure, which could have the same geological cause as the modeled one. Additional LOTEM measurements around this site would allow a satisfactory 3-D interpretation. Supplementary geophysical information in this area exists in form of MT and CSAMT measurements. The MT data at site "WIEL" (see figure 7.26) does not show any 3-D effect in the depth range of the LOTEM measurements (Hördt et al,

1991). Additional MT data and data from different geophysical measurements are either not available, or not directly comparable.

In the computations for the final model we used a resistivity of $0.1 \Omega\text{m}$, which is very low even for high salinity brine. Calculations with different resistivities and larger structures suggest that the resistivity of the structure could be higher, but not above $1 \Omega\text{m}$. An explanation of the low resistivity could be salty clay, which in addition to the decrease in resistivity may cause an induced polarization (IP) effect. IP effects on TEM data have been investigated by Flis et al. (1989) and by Smith and West (1989), who explained sign reversals in coincident loop TEM. To test the applicability of their theories to the LOTEM data in this area requires further measurements, such as geoelectric mapping, IP and shallow TEM to define more accurately the physical properties of the anomalous zone.

As our main conclusion we illustrate the possibility of quantitative interpretation of 3-D effects in LOTEM data which provides new and detailed information about the conductivity structure. In the Münsterland area, it is difficult to give a conclusive judgement about the geological truth of the model due to the sparse station density, but it is an excellent basis to design more detailed investigations.

Our interpretation approach can be applied in different areas, where the observed 3-D effect shows also a sign reversal at one receiver site together with an early time amplitude increase at other stations. In these cases we recommend the use of a thin-sheet program to obtain a first fit to the data. The second and third step will depend on the specific geologic situation, but the sequential use of simple and then more complex modeling routines may be reasonable in any case. Our procedure will not necessarily work if the observed 3-D effects are more complex than those shown here (i.e. the reversals are distributed over a large area). For these cases more experience with real field data is required.

SUMMARY CHAPTER 7

This chapter demonstrates with several case histories the successful application of the LOTEM method on different continents. For all case histories different hardware systems, processing and interpretation procedures and field crews were used. In Germany the objective of the survey was to obtain additional information between closely spaced wells in an area of extremely high cultural noise level and to interpret complex geology. In the United States several different systems were calibrated under known geology. In Australia a newly built field system was tested in an electromagnetically noisy environment under difficult field conditions (weather and accessibility).

In all cases the results are better than the expectations were before the survey. In the Ruhr Area survey the structure mapped with the LOTEM surveys matches with the known structure which is derived from numerous mines within the area. In Colorado the results from the three field systems turned out to be comparable although several data points had to be eliminated at the beginning because of irregularities in the sys-

tem response. During the field tests in Australia the LOTEM system confirmed that it could achieve a depth investigation of 1 to 2 kilometers and define geologic interfaces which were confirmed by other geophysical data and well logs.

Finally, three different 3-D numerical modeling routines are used to interpret LOTEM data from the Münsterland area, FRG. First, a thin-sheet algorithm gives the approximate strike direction of the structure. The second, an integral equation program, is used to explain the effect of the anomaly and its vertical extent. Last, a more realistic geological model is calculated using a finite difference algorithm. The combination of all three routines yields an interpretation strategy for complex structures.

PROBLEMS CHAPTER 7

1. Would we resolve the top of Carboniferous (Haltern case history) if directly above is a 100 m layer of Zechstein? Use the forward modeling program MODALL and high resistivities for the Zechstein.
2. How can you 'see' from the display of the inversion results and the importances the parameters are not highly correlated?
3. Calculate some representative curves for the DJ Basin case history including the weathering layer. What do you conclude from that?
4. Why do the deconvolved curves for the different receivers in the DJ Basin case history do not match?
5. Calculate comparative LOTEM synthetic curves for all the different models derived from the EM measurements for the Sydney Basin case history. Explain the differences and show which curves could also explain the LOTEM data.
6. Which is the range of applicability for the different 3-D programs used to interpret the Münsterland 3-D data?

KMS Technologies – KJT Enterprises Inc.
6420 Richmond Ave., Suite 610
Houston, Texas, 77057, USA
Tel: 713.532.8144

Please visit us
<http://www.kmstechnologies.com>

This material is not longer covered by copyright. The copyright was released by Elsevier to Dr. Strack on November 5th, 2007.

The author explicitly authorizes unrestricted use of this material as long as proper reference is given.